PLOS ONE

RESEARCH ARTICLE

Analytical comparability to evaluate impact of manufacturing changes of ARX788, an Anti-HER2 ADC in late-stage clinical development

Wayne Yu, Mysore P. Ramprasad*, Manoj Pal, Chris Chen, Shashi Paruchuri, Lillian Skidmore, Nick Knudsen, Molly Allen, Ying Buechler

Ambrx Incorporated, La Jolla, CA, United States of America

* mysore.ramprasad@ambrx.com, mrampras@yahoo.com

OPEN ACCESS

Citation: Yu W, Ramprasad MP, Pal M, Chen C, Paruchuri S, Skidmore L, et al. (2023) Analytical comparability to evaluate impact of manufacturing changes of ARX788, an Anti-HER2 ADC in late-stage clinical development. PLoS ONE 18(7): e0284198. https://doi.org/10.1371/journal.pone.0284198

Editor: Oksana Lockridge, University of Nebraska Medical Center, UNITED STATES

Received: March 24, 2023

Accepted: June 27, 2023

Published: July 10, 2023

Data Availability Statement: All relevant data are within the paper.

Funding: The authors received no specific funding for this work.

Competing interests: The authors have declared that no competing interests exist.

Abstract

ARX788 is an anti-HER2 antibody drug conjugate (ADC) developed using Ambrx proprietary Engineered Precision Biologics technology. The manufacturing process of ARX788 has been optimized during the course of early to late-phase clinical development. A comprehensive evaluation of side-by-side comparability between pre- and post-change process for ARX788 drug substance and drug product from a quality perspective was conducted based on ICH Q5E guidelines consisting of batch release assays, physicochemical and biophysical characterization, biological characterization, and forced degradation studies. All results have substantiated a high degree of similarity between the pre- and post-change ARX788 drug substance batches and drug product lots, demonstrating that the process manufacturing changes did not impact product quality.

Introduction

Antibody-drug conjugates (ADCs) are a class of therapeutics that combines an antigen-specific antibody backbone with a potent cytotoxic payload, resulting in an enhanced therapeutic index. The US FDA has currently approved 14 ADCs spanning several targets for hematological and solid tumors. The development of anti-human epidermal growth factor receptor 2 (HER2) agents has been one of the most meaningful advancements in the management of metastatic breast cancer, significantly improving survival outcomes [1]. Two anti-HER2 ADCs, Kadcyla® and Enhertu®, have been approved by the FDA in HER2-positive breast cancer. ARX788 is a next-generation, site-specific anti-HER2 ADC currently in global clinical trials for the treatment of HER2-positive metastatic breast cancer and gastric cancer [2–6]. It is comprised of a humanized HER2-targeting monoclonal antibody (mAb), conjugated to a cytotoxic tubulin inhibitor payload linker, Amberstatin (AS269), via a nonnatural amino acid incorporated into the two heavy chains of the antibody (as shown in Fig 1). Site-specific conjugation occurs when the hydroxylamine in AS269 reacts with the ketone group of the nonnatural amino acid, para-acetylphenylalanine (pAF), forming a highly stable oxime bond. This results in exactly two drug-linkers conjugated to each antibody molecule [2]. Further, this Ambrx Engineered Precision Biologics platform technology offers unique advantages of superior

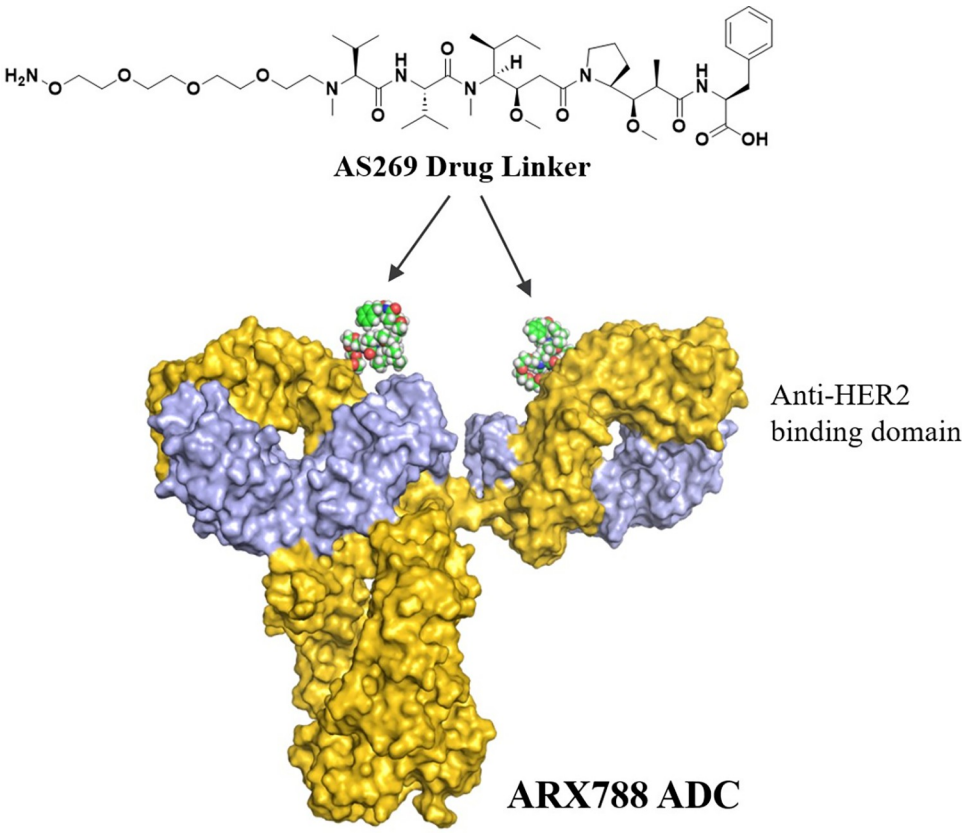

Fig 1. Schematic structure of ARX788. The cytotoxic payload, AS269, is conjugated to a nonnatural amino acid in the heavy chain of an anti-HER2 monoclonal antibody.

https://doi.org/10.1371/journal.pone.0284198.g001

efficacy, stability in systemic circulation, and a favorable safety profile as demonstrated in non-clinical studies with ARX788 [3].

Evaluating comparability of biologics due to manufacturing process changes from a quality perspective is based on the principles from ICH Q5E guidelines [7]. This assessment requires product-specific knowledge gathered through drug development to apply a totality-of-evidence approach to demonstrate comparability. Different levels of information are obtained from various studies including analytical studies for characterization of the molecule, animal studies for assessing toxicity, pharmacokinetics and pharmacodynamics, and clinical studies for assessing safety/tolerability, immunogenicity and efficacy. Analytical characterization of protein structure and function forms the foundation of comparability demonstration [8–11] which can independently avoid conducting expensive and time-consuming non-clinical and clinical studies [12]. Cutting-edge multi-level analytical and characterization tools for mAbs and ADCs to demonstrate comparability are well established in the literature [13–17], and forced-degradation studies further aid in teasing apart significant quality differences when performed side-by-side [18]. Setting suitable phase-appropriate acceptance criteria to compare batch-release specifications and biochemical, biophysical and biological analyses prior to performing the comparability study as well as utilization of statistical analysis is crucial to unbiased evaluation of the results [19–21].

Regulatory recommendation for ADC manufacturing involves rigorous control strategy and separate batch release of the cytotoxic payload and mAb intermediates, as well as the conjugated ADC drug substance (DS) and drug product (DP). Hence comparability studies need

to assess the risk and impact of manufacturing changes on product quality for each of the intermediates, as well as the final conjugated bulk DS and DP. Depending on the structure of the payload, its solubility and clearance during DS manufacturing, the impact of any changes in manufacturing of the cytotoxic payload linker on product quality of DS and DP also needs to be assessed. Furthermore, confirmatory clinical use compatibility studies of the drug product with ancillary components including closed system transfer devices (CSTDs) used to prepare and deliver the ADC need to be performed [22].

The manufacturing process of ARX788 involves conjugation of ARX788 mAb to AS269 in a controlled reaction environment with continuous mixing, followed by diafiltration into formulation buffer and 0.2 micron filtration, to produce the ADC drug substance which is then stored frozen at -70˚C. Drug Product manufacturing involves thawing the DS, mixing, sterile filtration and fill/finish of DS into glass vials and capping in an Isolator. This is followed by washing and drying of the drug product vials, visual inspection, and storage at -20˚C for the liquid formulation. For the new formulation and dosage form, the drug product vials are lyophilized and stoppered before storage at 2–8˚C. The manufacturing process of ARX788 DS and DP has undergone several changes during the life cycle from early to late-stage development which are summarized in Table 1. In this paper, we describe a comprehensive analytical comparability study between pre-change and post-change ARX788 materials to evaluate the impact of those changes, including manufacturing site change for DS and DP, and formulation and dosage form changes for DP. The mAb intermediate process did not undergo any significant changes, and thus did not warrant a separate comparability study. The AS269 intermediate underwent a minor change in manufacturing and was compared with pre-change lot using batch release and structural characterization methods.

Materials and methods

Ethics statement

No animal experiments were conducted in this study.

Her2 binding ELISA

An enzyme-linked immunosorbent assay (ELISA) was developed to measure ARX788 binding to target receptor HER2. Serially diluted ARX788 DS or DP samples were incubated in HER2-coated ELISA plates, and binding was detected with the addition of anti-human kappa-HRP antibody and incubation with 3,3',5,5'-Tetramethylbenzidine substrate. Sulfuric acid was

Table 1. Summary of ARX788 manufacturing changes for drug substance and drug product.

Item	Pre-Change	Post-Change
DS Manufacturer	Site A	Site B
DS Concentration	10 mg/mL	20 mg/mL
DS and DP formulation	X% Trehalose	X%+1.5% Trehalose
DP Dosage form	Frozen liquid	Lyophilized powder
DP Manufacturer	Site 1	Site 2
DP fill volume and Protein Amount	6 mL, 60 mg	2.625 mL, 52.5 mg
DP Container Closure	20 mL Schott glass 20 mm Bromobutyl Fluorotec stopper 20 mm Aluminum seal	10 mL Schott glass 20 mm Chlorobutyl Fluorotec Lyo stopper 20 mm Aluminum seal
DP Storage Temperature	-20˚C	2–8˚C

https://doi.org/10.1371/journal.pone.0284198.t001

added to stop the colorimetric reaction, and plates were read at absorbance wavelength 450 nm. The relative potency of pre-change or post-change ARX788 samples was calculated by comparison of its half-maximal effective concentration (EC50) value obtained from a 4-parameter sigmoidal fit of the dose response curve to the EC50 value of an ARX788 reference standard run on the same assay plate.

HCC1954 cytotoxicity assay

The functional activity of ARX788 is measured with a cytotoxicity assay. HER2-positive HCC1954 breast cancer cells are incubated with serially diluted ARX788 DS or DP samples for 3 days, and cellular viability is quantified with addition of CCK-8 reagent. Viable cells cleave CCK-8 to a colored formazan dye, which is measured by absorbance at wavelength 450 nm. The relative potency of pre-change or post-change ARX788 samples was calculated by comparison of its half-maximal inhibitory concentration (IC_{50}) value obtained from a 4-parameter sigmoidal fit of the dose response curve to the IC_{50} value of an ARX788 reference standard run on the same assay plate.

SEC-HPLC

Size variants of ARX788 DS and DP batches were analyzed by Size Exclusion Chromatography (SEC) on a TSKgel G3000SWXL column (Tosoh Bioscience, catalog no.: 05841) using an Agilent 1100 or 1200 HPLC system with UV detection at 280 nm. Samples were injected at 50 μg load and separation was achieved by an isocratic elution using a mobile phase consisting of 200 mM potassium phosphate, 250 mM potassium chloride, pH 6.0 at a flow rate of 0.5 mL/min and column temperature set at 25˚C. Percent area of High Molecular Weight species (HMW), monomer, and Low Molecular Weight (LMW) species were calculated using Agilent ChemStation Software.

CEX-HPLC

Cation Exchange chromatography (CEX) method was utilized to assess the charge variants of ARX788 DS and DP batches. Samples were loaded on a ProPac WCX-10, 4 x 250 mm column (Thermo Scientific) and eluted using a gradient of sodium chloride in a phosphate buffered mobile phase. Percent area of acidic, main, and basic species were calculated using Agilent ChemStation Software.

HIC-HPLC

Hydrophobic interaction chromatography (HIC) method was utilized to assess the drug to antibody ratio (DAR) of ARX788 DS and DP batches. Samples were loaded on a Butyl-NPR HPLC column (Tosoh) and eluted using a gradient of ammonium sulphate in a phosphate buffered mobile phase. The drug to antibody ratio was determined by calculating the peak area of the mAb (DAR0), 1-drug (DAR1), and 2-drug (DAR2) forms using the following equation:

$$\mathrm{DAR} = (\%\ 1{-}\mathrm{drug} + \%\ 2{-}\mathrm{drug}\ \mathrm{x}\ 2)/(\%\mathrm{mAb} + \%\ 1{-}\mathrm{drug} + \%\ 2{-}\mathrm{drug})$$

Free drug related impurities

ARX788 DS and DP batches were precipitated with acetonitrile in 2:3 ratio and vortexed for 1 minute. The samples were mixed on a thermomixer at room temperature and the mixtures were centrifuged for 30 minutes at 16,000 rcf. The supernatant was transferred to a new tube and mixed with hydroxylamine in a 1:1 ratio. The resulting solution was loaded to a XBridge Shield C-18 reverse phase column (Waters), followed by elution with a gradient of increasing

acetonitrile content in mobile phase. The flow rate was set at 0.8 ml/min and detection wavelength was set at 214 nm. The amount of residual free drug of AS269 in the tested sample is determined by interpolation of observed peak area against a standard curve. The results are reported as a weight percent of ARX788 ADC.

Intact mass determination

ARX788 DS samples were analyzed by LC-MS (Agilent 6200 Series TOF), following which molecular masses were obtained by deconvoluting the mass spectrum using Agilent MassHunter protein deconvolution software. For non-reduced mass analysis, no sample preparation was done prior to LC-MS analysis besides sample dilution in formulation buffer. For deglycosylation, the samples were treated with Peptide:N-Glycosidase F (PNGaseF) at 37˚C for 2 hours prior to LC-MS analysis. For reduced mass analysis, the samples were treated with dithiothreitol (DTT) along with 4 M guanidine hydrochloride (GdnHCl) and heated at 70˚C for 10 minutes before analysis by LC-MS.

All intact mass spectra were collected in positive ion mode with the mass range set to 700–3000 m/z with capillary and source temperatures at 300˚C, sheath gas flow rate at 50 arbitrary units and auxiliary gas flow rate at 8 arbitrary units. The capillary voltage was set to 3500V with the fragmentor voltage set to 200V. The acquired spectra were deconvoluted using Agilent MassHunter protein deconvolution software.

Peptide mapping

Peptide maps of ARX788 DS and DP samples were obtained using a Reversed Phase Ultra Performance Liquid Chromatography (RP-UPLC) method with UV detection. Approximately 200 μg of samples were denatured in pH 8 Tris buffered 6M GdHCl, and reduced in 20 mM DTT by heating at 56˚C for 30 min. The samples were allowed to cool to room temperature, and the reduced thiols were alkylated by incubation in 45 mM iodoacetamide in the dark for 30 min. The samples were then buffer exchanged using 0.5 mL Amicon Ultra 10 KDa MWCO spin-filters into trypsin digestion buffer containing 50mM TrisHCl pH 8, and 2M Urea. Sequencing grade Trypsin was then added, and the samples were incubated at 37˚C for 4 hours. To stop the reaction, 15μL of 20% TFA was added to each sample. Thereafter, 20μL volume of each sample were injected into a 4.6x150 mm Zorbax 300 SB-C8 (5μm) column and the peptides were separated using a gradient of TFA and acetonitrile at a flow rate of 1 mL/min and the UV spectra were acquired at 214 nm.

The disulfide bonds were mapped by comparing peptide maps of tryptic digests generated under non-reducing conditions. For reduced peptide mapping, all samples were denatured, reduced, and alkylated, followed by digestion with Trypsin. The digests were analyzed by RP-UPLC with UV detection.

icIEF

Imaged capillary iso-electric focusing (icIEF) was used to assess the pI and charge heterogeneity of ARX788 DS samples. Samples were prepared by adding and mixing appropriate amounts of carrier ampholytes, Urea, pI markers, arginine, and methylcellulose prior to analysis. The samples were loaded into the capillary and voltage applied, with pre-focusing condition at 1.5 kV for 2 minutes, and focusing condition at 3 kV for 8 minutes. Following the completion of focusing, a final image was taken at 280 nm for analysis. pI was calculated by comparing the position of the analyte to that of the pI standards. Percent main peak, acidic variants, and basic variants were also calculated based on area count of each species, relative to the total.

N-glycan analysis

The N-linked glycoforms of ARX788 DS batches were enzymatically released using PNGase F, and fluorescently labeled using 2-amino benzamide (2-AB). Excess 2-AB dye was removed using acetone precipitation, and a Speedvac was used to remove residual acetone. The 2-AB labeled glycans were then reconstituted in water and the N-glycan profiles of the DS batches were obtained by hydrophilic interaction liquid chromatography (HILIC) UPLC analysis followed by fluorescent detection.

Far UV circular dichroism

Far UV CD spectra (190 to 260 nm) of ARX788 DP lots were acquired using an Applied Photophysics Chirascan^{TM} Q100 Circular Dichroism Spectrometer containing a 0.01 cm cell at 20˚C. All samples were diluted in formulation buffer to obtain a protein concentration of 0.5 mg/mL before analysis. After subtracting the baseline spectrum, the CD spectra of the samples were converted to mean residue molar ellipticity (molar ellipticity per residue) curves using the sample concentration, the mean residue weight, and the path-length of the cell.

Near UV circular dichroism

ARX788 DP lots were diluted with formulation buffers to a concentration of 0.5 mg/mL before analysis. Near-UV (240 to 340 nm) CD measurements were carried out on an Applied Photophysics Chirascan^{TM} Q100 Circular Dichroism Spectrometer containing a 1 cm cell at 20˚C. After subtracting the baseline spectrum, CD spectra of the samples were converted to mean residue molar ellipticity (molar ellipticity per residue) using the sample concentration, the mean residue weight, and the path-length of the cell.

DSC

ARX788 DP lots were diluted to 1 mg/mL in formulation buffers and analyzed by MicroCal capillary VP Differential Scanning Calorimeter (DSC). The sample and reference cells were loaded with sample and formulation buffer, respectively. The instrument was programmed to scan from 10 to 110˚C at a rate of 1˚C/min, with a 10 second data averaging period and 15 min equilibration time. Buffer vs. buffer scans were recorded throughout the experiment sequence to obtain a baseline scan to subtract from the experimental data and to ensure the shapes of the baseline scans were reproducible over the course of the experiment. The raw data was processed using MicroCal PEAQ DSC software to calculate T_m values.

SEC-MALS

Fifty micrograms of ARX788 DP were analyzed by SE-HPLC (Agilent 1100 HPLC system) on a TSKgel G3000SWXL column with inline Multi Angle Light Scattering (MALS) detector (Wyatt DAWN HELEOS) to determine the size distribution and MW of the monomer and HMW peaks. Separation on SEC column was achieved using an isocratic gradient with a mobile phase containing potassium phosphate and potassium chloride pH 6.0. Flow rate was set to 0.5 ml/min with column temperature set at 25˚C. The SEC MALS data were analyzed using Astra v.7.3.2.

SV-AUC

ARX788 DP lots and reference were diluted 20-fold using formulation buffer to a final concentration of 0.5 mg/ml before analysis of Sedimentation Velocity-Analytical Centrifugation (SV-AUC) using a Beckman Coulter XL-I analytical ultracentrifuge with double sector

charcoal-filled Epon centerpiece. Protein sedimentation was accomplished through centrifugation at an angular velocity of 40,000 rpm. The concentration of each protein size variant was measured as a function of time and radial position using absorbance (A280) to monitor sedimentation. The concentration profiles were subsequently analyzed and plotted as a c(s) distribution.

ADCC effector function

HER2-expressing SK-BR-3 cells were seeded at 5,000 cell/well in a 96-well assay plate, incubated overnight, and the growth medium was aspirated and replaced with 25 uL/well assay buffer (RPMI-1640+4% Low IgG Serum). Serially diluted ARX788 samples were added to the assay wells, followed by addition of 25 uL/well of Antibody Dependent Cellular Cytotoxicity (ADCC) Bioreporter Cells (Promega cat# G7010). The ADCC Bioreporter cells are engineered Jurkat cells stably expressing FcγRIIIa V158 (high affinity) receptors on the cell surface and an NFAT response element driving expression of firefly luciferase. After incubating assay plates for 6 hours at 37˚C and 5% CO_2, Bio-Glo Luciferase Assay Reagent was added, incubated for 30 minutes protected from light, and luminescence was measured on a SpectraMax plate reader.

The relative potency of ARX788 samples was calculated by comparison of its half-maximal effective concentration (EC_{50}) values obtained from a 4-parameter sigmoidal fit of dose response curves against the EC_{50} value of the ARX788 reference standard run in the same assay plate.

Fc receptors binding and FcRn binding by Octet

The binding of ARX788 to Fc gamma receptors CD64 (FcγRI), CD32a (FcγRIIA) and CD16a (FcγRIIIA) was measured in a biolayer interferometry assay on an Octet RED96 system (Sartorius). Streptavidin-coated biosensors were loaded with purified biotinylated human CD64, CD32a, or CD16a in HBS-P+ buffer (Cytiva). After washing biosensors with HBS-P+ buffer to remove unbound protein, serially diluted ARX788 drug substance in HBS-P+ buffer was monitored for association and dissociation kinetics with loaded biosensors. Data were referenced using a parallel buffer blank subtraction. The processed binding curves were globally fitted using the Langmuir model describing a 1:1 binding stoichiometry. To avoid avidity effects in the CD32a and CD16a assays, the binding curves were globally fitted using 3.0 seconds for the dissociation step with the Langmuir model. Likewise, the FcRn binding assay was measured in a biolayer interferometry assay on an Octet RED96 system (Sartorius). Streptavidin-coated biosensors were loaded with purified biotinylated human FcRn in pH 6.0 assay buffer (100mM sodium phosphate, 150mM sodium chloride, 0.05% (v/v) Tween 20, pH 6.0). After washing biosensors with assay buffer to remove unbound protein, serially diluted ARX788 drug substance in pH 6.0 assay buffer was added and monitored for association and dissociation kinetics with FcRn loaded biosensors. Data were referenced using a parallel buffer blank subtraction. To avoid avidity effects, the processed binding curves were globally fitted using 3.0 seconds for the dissociation step with the Langmuir model describing a 1:1 binding stoichiometry.

Results and discussions

Side-by-side batch analysis

The batch release data of the pre-change and post-change DS and DP batches were compared side by side as shown in Table 2 and Table 3, respectively. For DS batches, all the purity assays

Table 2. Bulk drug substance batch release analysis of pre-change and post-change batches.

Tests		Pre-Change	Post-Change 1	Post-Change 2	Post-Change 3
Peptide map		Conforms to RS	Conforms to RS	Conforms to RS	Conforms to RS
pH		6.0	6.0	6.0	6.0
Osmolality, mOsmol/kg		157	210	209	209
Protein concentration, mg/mL		10.1	20.0	19.1	20.7
HER2 Binding ELISA % relative to Reference		98	125	117	107
HCC1954 Cytotoxicity Assay, % relative to Reference		106	96	90	74
SEC-HPLC	Main %	99.3	99.6	99.6	99.6
	HMW %	0.6	0.4	0.4	0.4
	LMW %	0.2	ND	ND	ND
CEX-HPLC	Main %	50.3	51.9	49.2	48.7
	Acidic %	33.6	29.4	29.5	30.3
	Basic %	16.1	18.6	21.3	21.0
CE-SDS (NR) % purity		95.1	96.9	97.7	98.1
CE-SDS (R) % purity		96.9	97.7	97.2	96.9
HIC-HPLC	DAR	1.9	1.9	1.9	1.9
	mAb	ND	0.5	ND	ND
	Impurity	5.4	3.8	4.2	4.0
Free drug related impurities w/w		< 0.016% (LOQ)	0.016%	0.042%	0.028%

DAR = Drug antibody ratio; LOQ = limit of quantitation; NA = not tested; ND = not detected; RS = Reference Standard

https://doi.org/10.1371/journal.pone.0284198.t002

including SEC-HPLC, CEX-HPLC, Capillary Electrophoresis-Sodium Dodecyl Sulfate Non-Reduced and Reduced (CE-SDS NR and R), and HIC-HPLC showed similar results. Likewise, the potency assays including HER2 Binding ELISA and HCC1954 Cytotoxicity Assay also showed similar results except for the first DS post-change batch ELISA at 125% and third post-change batch cytotoxicity at 74%, which is likely due to assay variability since the corresponding DP lot's ELISA and cytotoxicity results are 94% and 103% (see Table 3), respectively. The protein concentration was increased from 10 mg/mL to 20 mg/mL in the post-change lots to reduce lyophilization cycle time during DP manufacturing. Trehalose concentration was also increased by 1.5% to help improve the stability of the drug product. These two changes accounted for the increase in osmolality from ~157 to 210 mOsmol/kg. Likewise, the DP lot release analysis yielded similar results in most assays except for the expected differences in protein concentration and osmolality (3). In summary, both pre- and post-change DS and DP batches passed the acceptance criteria for batch release and showed similar results.

Side-by-side physicochemical analysis

A panel of physicochemical tests were conducted for both pre- and post-change BDS batches including intact mass analysis under both non-reducing and reducing conditions, peptide mapping, icIEF, and N-glycan analysis. Analytical methods and target acceptance criteria for assessing product comparability between pre-change and post-change DS and DP batches manufactured for clinical development were pre-determined before the execution of the study.

Intact mass analysis, non-reduced

ARX788 DS was analyzed by LC-MS (Agilent 6200 Series TOF), following which molecular masses were obtained by deconvoluting the mass spectrum using Agilent Protein Deconvolution software. The deconvoluted spectra of DS obtained from pre-change and post-change 1

Table 3. Drug product lot release analysis of pre-change and post-change lots.

Tests		Pre-Change	Post-Change 1	Post-Change 2	Post-Change 3
Appearance		Colorless and clear liquid	Colorless and clear liquid	Colorless and clear liquid	Colorless and clear liquid
Post thaw/ Reconstitution)		EFVP	EFVP	EFVP	EFVP
Cake Appearance		NA	White cake, no meltback or collapse	White cake, no meltback or collapse	White cake, no meltback or collapse
Reconstitution Time (3 vials)		NA	2 min, 07s	2 min, 11s	1 min, 55s
			2 min, 11s	2 min, 05s	2 min, 01s
			2 min, 05s	2 min, 15s	1 min, 59s
Moisture Content		NA	0.20%	0.20%	0.20%
Peptide map		Conforms to RS	Conforms to RS	Conforms to RS	Conforms to RS
pH		5.9	5.9	5.9	6.0
Osmolality, mOsmol/kg		153	202	199	204
Protein Concentration, mg/mL		10.3	NA	NA	NA
Protein Content/Vial		NA	101%	96%	105%
HER2 binding ELISA, % of RS		89	94	95	97
HCC1954 Cytotoxicity Assay, % of RS		86	99	97	103
SEC-HPLC	Main %	99.3	99.5	99.5	99.5
	HMW %	0.6	0.5	0.5	0.5
	LMW %	0.1	0.0	0.1	0.0
CEX-HPLC	Main %	50.0	49.5	51.4	52.1
	Acidic %	34.0	29.7	29.8	29.1
	Basic %	16.0	20.7	18.8	18.8
CE-SDS, NR (Main), % purity		96.0	95.9	95.4	95.7
CE-SDS, R (LC + HC), % purity		97.1	97.0	97.4	97.5
HIC-HPLC	DAR	1.9	1.8	1.8	1.8
	mAb	ND	ND	ND	ND
	Impurity	4.5	3.5	4.1	4.5
Free drug related impurities, w/w		<0.02%	0.01%	0.03%	0.02%

EFVP = Essentially free of visible particles; NA = not applicable; ND = not detected; RS = Reference Standard

https://doi.org/10.1371/journal.pone.0284198.t003

materials as well as the Reference Standard (RS) are shown in Fig 2A. The measured molecular masses showing different glycan forms are listed in Table 4. Taking the results from the reference standard for example, the most abundant species observed at 150047.56 Da is the ADC containing the N-glycosylation G0F on both heavy chains. The species observed at 150215.37 Da corresponds to the ADC containing an N-glycan G0F and G1F, while the ADC containing a combination of either G0F and G2F or two G1F glycans corresponds to the species observed at 150368.29 Da.

The molecular masses of all batches of DS are consistent with the theoretical values and the similarity of results indicate that all batches are comparable.

The deconvoluted spectra of reduced DS batches obtained from pre-change and post-change are shown in Fig 2B for heavy chain. The measured molecular masses of light chain and heavy chain observed in both batches are listed in Table 5. The results are consistent with the theoretical values and the similarity of results indicate the batches are comparable.

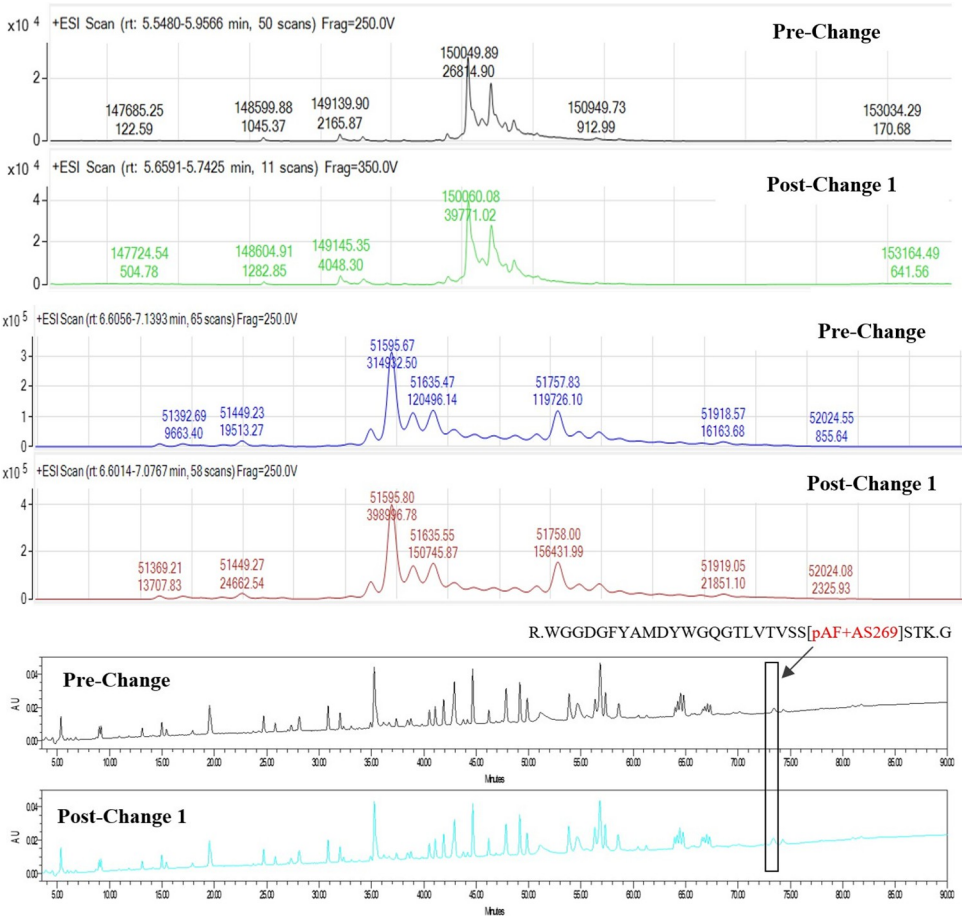

Fig 2. A) Non-reduced Deconvoluted Mass Spectra of ARX788 Drug Substance Batches, B) Reduced Deconvoluted Mass Spectra of Heavy Chains in ARX788 Drug Substance, and C) 214 nm UV Profiles of ARX788 Drug Substance Trypsin Digest Peptide Map.

https://doi.org/10.1371/journal.pone.0284198.g002

Peptide mapping

ARX788 DS samples were analyzed by peptide mapping to confirm the comparability of their primary sequences. All samples were denatured, reduced, and alkylated, followed by digestion with Trypsin. The digests were analyzed by RPHPLC with UV 214 detection. The peptides were well resolved and provided comparable UV profiles of pre-change and post-change1 as shown in Fig 2C. The para-acetyl phenylalanine (pAF) and AS269 containing peptide highlighted in the chromatograms was also observed in all batches with comparable peak intensities. These results indicate that all batches of ARX788 DS are chemically comparable.

Imaged capillary isoelectric focusing (icIEF)

icIEF electrophoresis method separates proteins based on differences in isoelectric point (pI) using a pH gradient formed from ampholytes in an electric field. The pI value of the protein is determined by comparing against two pI standard markers. ARX788 DS batches from pre-change and post-change were analyzed using ProteinSimple Imaged icIEF system with a fluorocarbon-coated electrophoresis capillary for the determination of pI and detection of charge variants. As shown in Fig 3A, the UV profiles of all batches of ARX788 DS were highly similar

Table 4. Molecular mass of ARX788 drug substance.

Sample	Modifier	Measured Mass (Da)	Mass Difference relative to Pre-Change Sample (Da)
Pre-Change	G0F/G0F	150049.89	NA
	G0F/G1F	150206.23	NA
	G1F/G1F or G0F/G2F	150367.56	NA
Post-Change 1	G0F/G0F	150060.08	10.19
	G0F/G1F	150220.66	14.43
	G1F/G1F or G0F/G2F	150375.91	8.35
Post-Change 2	G0F/G0F	150058.12	8.23
	G0F/G1F	150219.68	13.45
	G1F/G1F or G0F/G2F	150375.53	7.97
Post-Change 3	G0F/G0F	150062.02	12.13
	G0F/G1F	150222.69	16.46
	G1F/G1F or G0F/G2F	150374.61	7.05
Reference Standard	G0F/G0F	150047.56	-2.33
	G0F/G1F	150215.37	9.14
	G1F/G1F or G0F/G2F	150368.29	0.73

Note: G0F, G1F, G2F are the different types of biantennary N-glycans attached to the conserved Asn297 residue in the heavy chain where G# refers to the number of Galactose residues and F stands for fucosylation of the initial GlcNAc (N-Acetylglucosamine) residue.

https://doi.org/10.1371/journal.pone.0284198.t004

Table 5. Molecular mass of reduced ARX788 drug substance.

Sample	Modifier	Measured Mass (Da)	Mass Difference relative to Pre-Change Sample (Da)
Pre-Change	LC	23444.20	NA
	HC:AS269:G0F	51595.67	NA
	HC:AS269:G1F	51757.83	NA
	HC:AS269:G2F	51918.57	NA
Post-Change 1	LC	23444.28	0.08
	HC:AS269:G0F	51595.80	0.13
	HC:AS269:G1F	51758.00	0.17
	HC:AS269:G2F	51919.05	0.48
Post-Change 2	LC	23444.23	0.03
	HC:AS269:G0F	51595.73	0.06
	HC:AS269:G1F	51757.79	-0.04
	HC:AS269:G2F	51918.51	-0.06
Post-Change 3	LC	23444.28	0.08
	HC:AS269:G0F	51595.95	0.28
	HC:AS269:G1F	51758.09	0.26
	HC:AS269:G2F	51918.43	-0.14
Reference Standard	LC	23444.05	0.08
	HC:AS269:G0F	51595.49	0.13
	HC:AS269:G1F	51757.60	0.17
	HC:AS269:G2F	51918.00	0.48

Note: G0F, G1F, G2F are the different types of biantennary N-glycans attached to the conserved Asn297 residue in the heavy chain where G# refers to the number of Galactose residues and F stands for fucosylation of the initial GlcNAc (N-Acetylglucosamine) residue. LC and HC refers to the light chain and heavy chain of the antibody respectively.

https://doi.org/10.1371/journal.pone.0284198.t005

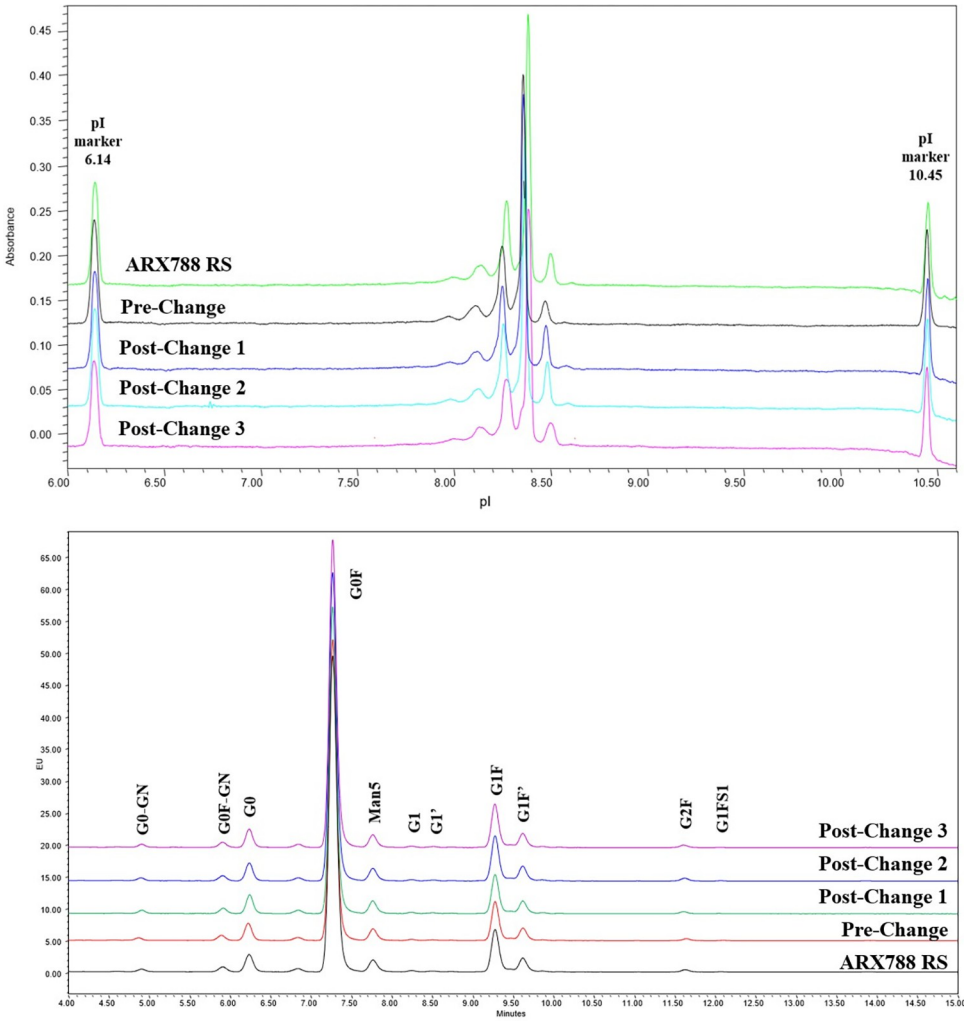

Fig 3. A) Imaged Capillary Isoelectric Focusing Electropherograms and B) HILIC-FL Profile of 2-AB Labeled N-Glycans from ARX788 DS batches.

https://doi.org/10.1371/journal.pone.0284198.g003

and displayed a main peak pI value of 8.4. The relative percentage of charge variants were also similar among the batches (Table 6) with 0.7% difference in main peak purity between Pre-change and post-Change2 batches. Overall, these results indicate a high level of comparability among the batches of ARX788 DS.

Table 6. Isoelectric point and relative abundance of charge variants in ARX788 dug substance determined by icIEF.

Sample	pI	% Acidic	%Main	% Basic
Reference Standard	8.4	42.5	49.1	8.4
Pre-Change	8.4	43.4	48.7	7.9
Post-Change 1	8.4	39.4	49.3	11.3
Post-Change 2	8.4	39.7	49.4	11.0
Post-Change 3	8.4	41.2	49.2	9.6

https://doi.org/10.1371/journal.pone.0284198.t006

Table 7. Relative abundance of N-glycan forms in ARX788 drug substance.

Sample	Relative Abundance (%)						
	G0	G0F	G1F	G1	G2F	Man5	Other
Pre-Change	4.2	74.0	13.4	0.6	0.5	3.2	4.1
Post-Change 1	4.3	73.8	13.4	0.6	0.5	3.5	3.8
Post-Change 2	4.1	72.3	15.0	0.7	0.8	3.4	3.7
Post-Change 3	4.2	72.8	14.5	0.7	0.7	3.4	3.7
Reference Standard	4.1	73.9	14.1	0.6	0.7	3.2	3.4

Note: G0, G0F, G1, G1F, G2F = biantennary N-glycan where G# refers to the number of Galactose residues and F stands for fucosylation of the initial GlcNAc (N-Acetylglucosamine) residue. Man5 refers to N-linked manose-5 glycan.

https://doi.org/10.1371/journal.pone.0284198.t007

N-glycan analysis

The N-linked glycoforms of ARX788 DS batches were enzymatically released using PNGase F and fluorescently labeled using 2-amino benzamide (2-AB). The N-glycan profiles of the DS batches were obtained by using hydrophilic interaction liquid chromatography (HILIC) UPLC analysis and fluorescent detection (excitation at 330 nm and emission detected at 420 nm). The N-glycan profiles for all four batches of DS and reference are shown in Fig 3B and the results are summarized in Table 7. The results show that the most abundant N-glycan forms are G0, G0F, Man-5, G1, G1F, and G2F and the glycan profiles are almost identical indicating a high degree of comparability among the DS batches from pre-change and post-change.

Side-by-side biophysical characterization

Various biophysical tests were conducted for both pre- and post-change DP lots. Far UV CD was employed for secondary structure comparison while near UV CD and DSC were carried out for tertiary structure comparison. The size distributions of ARX788 DP lots were compared using two different biophysical techniques, namely SEC-MALS, and SV-AUC.

Secondary structural comparison

Far UV CD was employed to assess the secondary structure element of these samples. The overlaid mean residue molar ellipticity (MRME) results are presented in Fig 4A and the spectra are identical within experimental error, which shows that the relative composition of secondary structural elements are highly comparable. These results demonstrate a high degree of spectral similarity indicating lot-to-lot consistency of secondary structure.

Tertiary structural comparison

The near UV CD determines the tertiary structure due to asymmetric environments of tryptophan, tyrosine, phenylalanine, and disulfide. The spectra are shown in Fig 4B, which shows a high degree of similarity between pre-change and post-change drug product lots demonstrating their comparability at the level of tertiary structure. Likewise, Capillary differential scanning calorimetry (DSC) was employed to detect the thermal transition temperature (Tm) of proteins for thermal and conformational stability determination. Proteins with different thermal stabilities show different Tm values that reflect their higher order folded structures. The DSC thermograms of the drug product lots along with reference are shown in Fig 4C. The first transition (T_m1) represents the melting of C_H2 domain of the heavy chain and the second transition (T_m2) represents the melting of Fab and C_H3 domains. The overlaid thermogram shows that both the peak shape and transition temperatures are nearly identical. The results

demonstrate that pre-change and post-change Lyo ARX788 DP materials have the same T_m values and are therefore comparable.

Size comparison by SEC-MALS

ARX788 DP lots were analyzed by SE-HPLC with inline MALS detector to determine the size distribution and MW of the monomer and HMW peaks. The results are shown in Fig 4D. All four batches of ARX788 drug product show identical 153-155kD MW for the monomer peak. The MW of HMW species in these samples also correlate roughly with that of a dimer of the main peak considering higher variability of MW determination because of low abundance (signal) of the HMW peak.

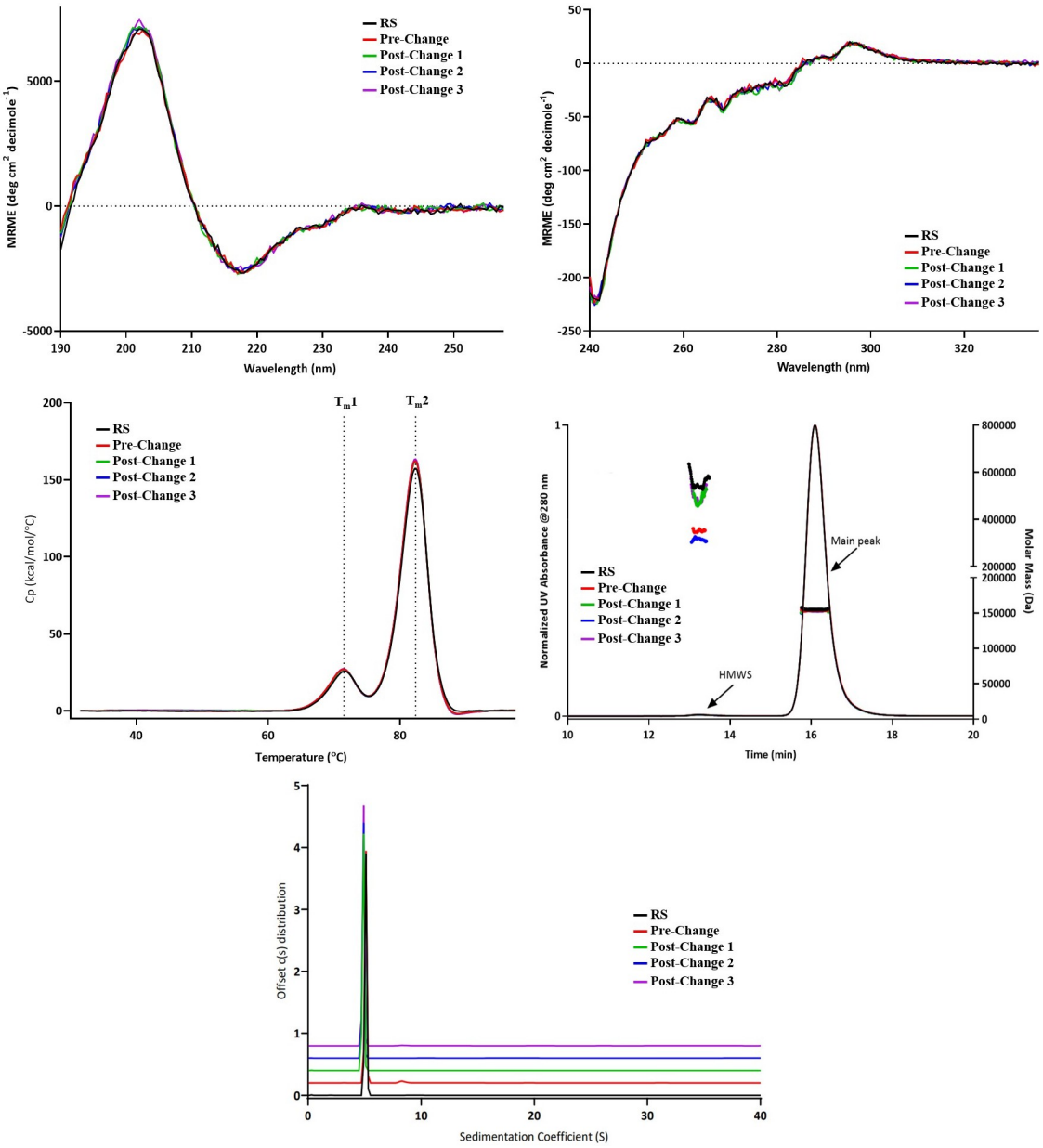

Fig 4. Biophysical Characterization of ARX788 DP lots: A) Far UV CD spectra, B) Near UV CD spectra, C) DSC thermograms, D) SEC-MALS chromatograms, and E) SV-AUC c(s) distribution plot.

https://doi.org/10.1371/journal.pone.0284198.g004

Size comparison by SV-AUC

Sedimentation velocity (SV) measurement by analytical ultracentrifugation (AUC) is a classical method for protein size analysis and state of association or aggregation. Aggregates can be detected based on difference in sedimentation coefficients which is a function of shape and mass of the oligomers. ARX788 DP lots were compared using SV-AUC and the resulting plot of c(s) distribution is presented in Fig 4E. The sedimentation coefficients of the main peak are slightly different between pre-change and the 3 lots of post-change DP. This difference is due to the fact that the formulation buffer of the latter samples contains slightly higher Trehalose concentration, which leads to an increase in viscosity and density, thus lowering the sedimentation rate of post-change samples. The data also suggest that pre-change may contains slightly higher HMW species although it is difficult to quantitatively assess the difference as the values were below detection threshold of 3.7% (note that SE-HPLC as well as SEC-MALS show very similar HMW levels). Based on these results, it is concluded that theses samples have comparable size distributions by SV-AUC, showing $>$96% main peak and $\leq$3.1% HMW species for all DP lots.

Side-by-side biological characterization

ADCC functional activity comparison. Although not the primary mechanism-of-action of ARX788, ADCC activity of pre-change and post-change batches were measured in an ADCC reporter assay Representative dose response curves for ARX788 reference standard, DS Pre-change batch, and DS Post-change batches 1 and 2, are shown in Fig 5A and the average Relative Potency and fold difference values are summarized in Table 8. The 1.17 to 1.42-fold-difference in Relative Potency of ARX788 DS post-change versus pre-change batches fell within the variability of the assay and met the defined difference in relative potency criterion. Thus, the observed ADCC activity is comparable between ARX788 DS pre-change and post-change batches.

Fc receptor affinity comparison

An orthogonal method for analyzing effector function is by examining the binding affinity of ARX788 from pre- and post-change batches towards Fc gamma receptors including CD64 (FcγR I), CD32a (FcγR IIA), CD16a (FcγR IIIA). The binding kinetics sensorgrams of pre-change and post-change1 DS to the three Fc gamma receptors are shown in Fig 5B and the dissociation constants (KD) of all samples are summarized in Table 9. Pre-change and post-change DS samples showed highly similar binding kinetics for the three tested Fc gamma receptors as seen in the sensorgrams, which suggested that these samples have similar affinities towards the receptors. Indeed, the KD values are highly similar between RS to pre-change as well as RS to post-change batches (KD ratios are very close to 1.00). Thus, the Fc gamma binding characteristics are comparable among the four DS batches.

Analysis of FcRn binding by ARX788 should also provide insight into effector function comparability. The binding kinetics sensorgrams of pre-change and post-change1 DS to FcRn receptor are shown in Fig 5C and the dissociation constants (KD) of all samples are summarized in Table 9. All pre-change and post-change DS samples showed highly similar binding kinetics for FcRn receptor as seen in the sensorgrams, which suggested that these samples have similar affinities towards the receptors. Indeed, the KD values are highly similar between RS to pre-change as well as RS to post-change batches (KD ratios very close to 1). Thus, the FcRn binding affinities are comparable among the four DS batches.

Side-by-side forced degradation study

To ascertain comparative stability and comparability under thermal stress, DP lots were incubated at an elevated temperature of 40˚C for 1, 2, and 4 weeks in an upright position of the

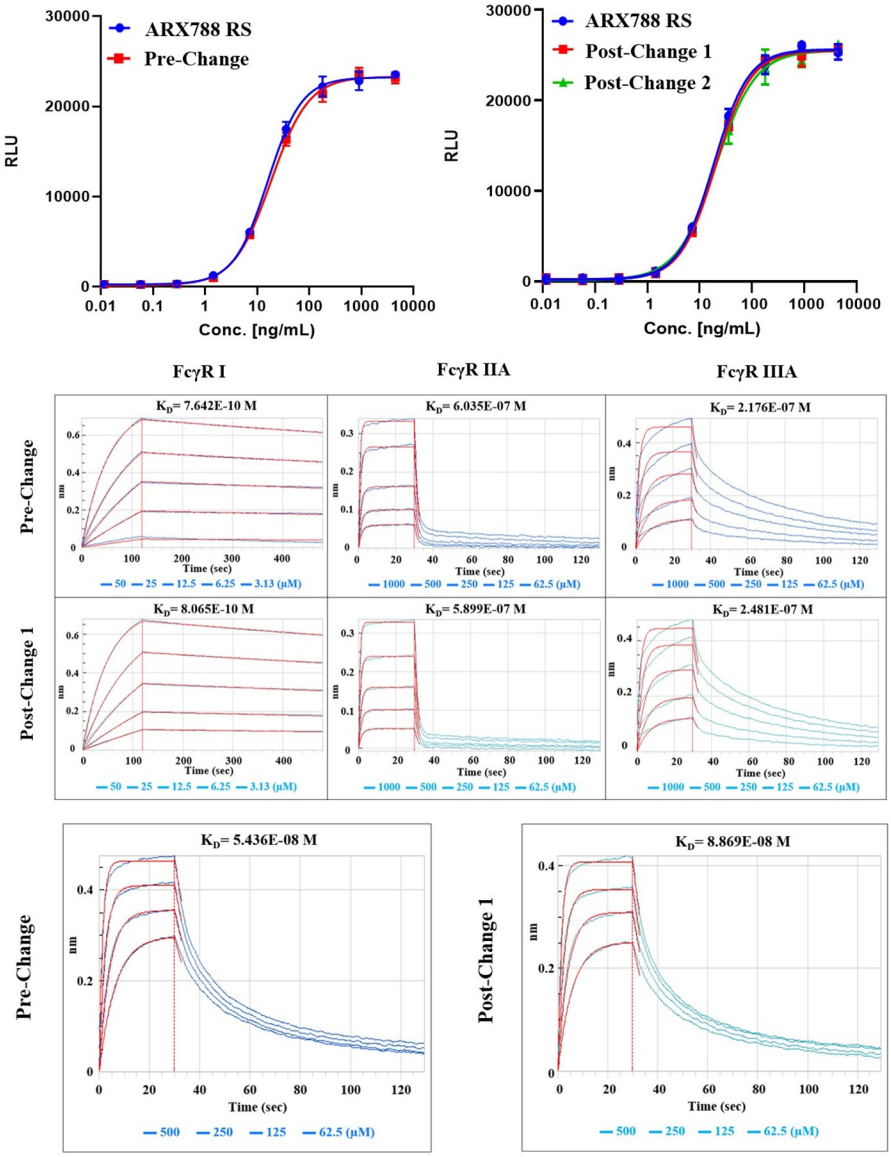

Fig 5. Side-by-side effector function characterization of ARX788 DS batches: A) ADCC Dose Response Curves, B) Fc gamma Receptors Binding Kinetics Sensorgrams, and C) FcRn Receptors Binding Kinetics Sensorgram.

https://doi.org/10.1371/journal.pone.0284198.g005

Table 8. Average fold difference in relative ADCC potency of ARX788 DS batches.

Sample	Average Relative Potency (%)	% CV	Average Fold Difference in Relative Potency (vs Pre-Change)
Pre-Change	87.4	2.9	1.00
Post-Change 1	102.0	12.2	1.17
Post-Change 2	103.3	11.0	1.18
Post-Change 3	123.8	6.3	1.42

https://doi.org/10.1371/journal.pone.0284198.t008

Table 9. Fc Gamma and FcRn receptors binding affinities for ARX788 DS batches.

Sample	CD64 K_D Ratio (Sample/RS)	CD32a K_D ratio (Sample/RS)	CD16a K_D Ratio (Sample/RS)	FcRn K_D Ratio (Sample/RS)
Reference Standard	NA	NA	NA	1.00
Pre-Change	1.00	1.28	0.99	0.98
Post-Change 1	1.05	1.25	1.13	1.60
Post-Change 2	0.98	1.22	1.03	1.33
Post-Change 3	0.89	1.05	1.01	1.19

https://doi.org/10.1371/journal.pone.0284198.t009

vials. Prior studies of forced degradation including freeze/thaw, agitation, and thermal stress had indicated only thermal stress as the most aggressive stress condition. Therefore, only thermal stress condition was used in the comparability study. Since the pre-change DP is in liquid form while post-change DP is lyophilized powder, a set of post-change1-3 DP vials were reconstituted at T0 to ~10 mg/mL (same concentration as pre-change DP) and then incubate as liquid DP together with pre-change DP at 40˚C with 75±5% relative humidity, to ensure a fair comparison for the forced degradation study. Another set of post-change1-3 DP vials were incubated under the same thermal stress condition without reconstitution to determine if the lyophilized dosage form would improve ARX788 DP stability. The degradation profiles of ARX788 DP lots were then determined by a side-by-side comparison of key quality attributes using stability indicating batch release analytical and biological assays (latter not shown). In addition, the T0 data in the forced degradation study allowed assessment of the side-by-side batch release testing requirement in ICH Q5E guidance. Only representative data from the Pre-change vs. Post-change Lyo 1 batch are shown (Fig 6A and 6B).

CEX-HPLC

The level of charge heterogeneity in both lots of thermally stressed drug product from pre-change and post-change was determined by CEX-HPLC. The magnified CEX chromatograms of pre-change, reconstituted post-change Lyo 1 and post-change Lyo 1 are shown in Fig 6A. A clear trend in reduction of main peak purity and concomitant appearance of acidic and basic species for both pre-change and reconstituted post-change Lyo 1 can be observed, while the lyophilized post-change DP purity remains unchanged. From the chromatograms, it can also be observed that the rates of change were very comparable. Overall, this indicates that the drug product lots from both Pre-change and Post-change Lyo (after reconstitution) degrade similarly when thermally stressed at 40˚C and signifies a high degree of similarity of the ADC between these two Processes. Post-change Lyo DP in its lyophilized state is resistant to this degradation, which shows the improved stability of this new dosage form.

SEC-HPLC

The level of HMW, monomeric, and LMW species of the thermally stressed drug product was determined by SE-HPLC. The magnified SEC chromatograms of control samples (T0) and all three timepoints are shown in Fig 6B. Pre-change and reconstituted Post-change samples both showed a similar gradual increase in LMW. Drug product from both Pre-change and Post-change Lyo show identical trend with gradual drop in main peak purity and increase in LMW levels indicating high degree of comparability between these two processes. Post-change in its lyophilized state is resistant to this degradation, which shows the improved stability of this new dosage form.

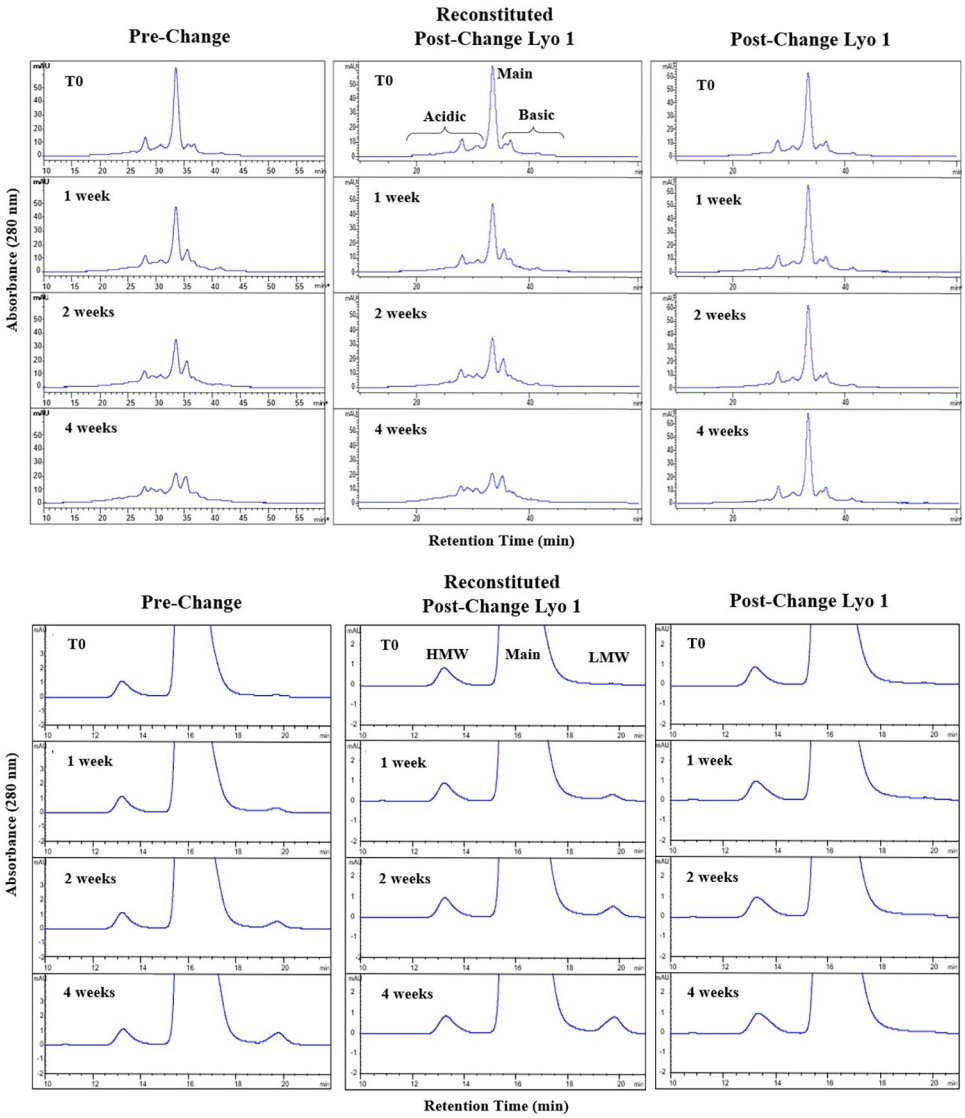

Fig 6. Side-by-side forced degradation purity analysis of ARX788 DP lots by A) CEX HPLC, B) SEC HPLC.

https://doi.org/10.1371/journal.pone.0284198.g006

HIC-HPLC

The drug to antibody ratio (DAR), along with the unconjugated mAb, 1-drug, 2-drug, and impurities in the thermally stressed (up to 4 weeks at 40˚C) drug product lots were determined by HIC-HPLC. The data are shown in Table 10. The results show that after 4 weeks of thermal stress, Pre-change and reconstituted Post-change 1 Lyo drug product lots show a small increase in relative abundance of DAR1 species and a minute decrease in the relative abundance of DAR2 species indicating gradual loss of the AS269 drug. These results correlate well with free drug assay results where a minute increase in free drug was observed under identical forced degradation conditions, namely 4 weeks at 40˚C (see below). The nominal DAR for all lots of thermally stressed DP however remains the same (1.9), as the changes were very small. The high degree of similarity in the HIC-HPLC results indicate that the drug-antibody conjugate profile and stability of the Pre-change and Post-change lot after reconstitution, are comparable. The non-reconstituted Post-change lots are resistant to this degradation and the free

Table 10. Calculated DAR of thermally stressed ARX788 drug product by HIC-HPLC.

Sample	species	T0	Week 1	Week 2	Week 4
Pre-Change	% mAb	0.2	0.2	0.3	0.3
	% 1-Drug	8.1	8.9	9.1	10.7
	% 2-Drugs	85.4	85.4	85.6	83.8
	% Impurities	6.2	5.6	5.0	5.2
	DAR	1.9	1.9	1.9	1.9
Post-Change 1—Reconstituted	% mAb	0.3	0.3	0.4	0.5
	% 1-Drug	11.0	11.6	11.7	13.1
	% 2-Drugs	83.0	83.3	83.1	81.6
	% Impurities	5.7	4.8	4.7	4.8
	DAR	1.9	1.9	1.9	1.9
Post-Change 1 -Lyophilized DP	% mAb	0.3	0.3	0.5	0.4
	% 1-Drug	11.0	11.0	10.6	10.8
	% 2-Drugs	83.0	83.6	83.6	84.0
	% Impurities	5.7	5.1	5.4	4.8
	DAR	1.9	1.9	1.9	1.9

https://doi.org/10.1371/journal.pone.0284198.t010

drug assay also shows that there is no increase in free drug levels (see below). These data also show that the oxime bond that conjugates the drug linker payload, AS269, to the antibody is very stable under heat stress in the lyophilized DP.

Residual free drug analysis

The level of free drug impurity in thermally stressed ARX788 drug product lots was determined by RP-HPLC assay as described in the Materials and Methods section. The amount of free drug (shown as calculated % weight of free drug per weight of ADC) for Pre-change, Post-Change 1 DP reconstituted, and Post-Change 1 Lyophylized DP are listed in Table 11. The data show that both Pre-Change and reconstituted Post-Change 1 DP demonstrate a similar slow rate of increase in level of free drug. This indicates that when subjected to thermal stress at 40˚C, the pre-change and post change DP lots degrade in a similar manner, demonstrating a high degree of comparability. Post-Change DP in the lyophilized state before reconstitution is resistant to this degradation, which demonstrates the improved stability of this new dosage form.

Overall, the forced degradation profiles assessed using stability indicating analytical assays of DP from pre-change and post-change batches at 40˚C were highly similar.

Conclusion

In summary, side-by-side comparison of pre-change and post-change Drug Substance and Drug Product was conducted by evaluating different chemical, biochemical and biological functions and also included a comparison of degradation profiles under thermal stress

Table 11. Free drug impurity in thermally stressed ARX788 drug product.

Sample	T0	Week 1	Week 2	Week 4
Pre-Change	<0.016	<0.016	0.023	0.032
Post-Change 1—Reconstituted	<0.016	0.020	0.026	0.037
Post-Change 1 -Lyophilized DP	<0.016	<0.016	<0.016	<0.016

https://doi.org/10.1371/journal.pone.0284198.t011

conditions. All results have demonstrated a high degree of similarity between the pre- and post- manufacturing change ARX788 materials. Therefore, it is anticipated that the changes made to optimize the ARX788 manufacturing process will not adversely impact product quality, safety, pharmacokinetics, potency, and efficacy.

Acknowledgments

The Authors thank Ji Young Kim for her supervision of the ADCC effector function analysis, and Karen Cha for her expert guidance on global regulatory submissions.

Author Contributions

Conceptualization: Wayne Yu, Mysore P. Ramprasad, Ying Buechler.

Data curation: Wayne Yu, Manoj Pal, Chris Chen, Shashi Paruchuri, Lillian Skidmore, Nick Knudsen, Molly Allen.

Formal analysis: Wayne Yu, Manoj Pal, Chris Chen, Shashi Paruchuri, Lillian Skidmore, Nick Knudsen, Molly Allen.

Investigation: Wayne Yu, Mysore P. Ramprasad, Manoj Pal.

Methodology: Wayne Yu, Manoj Pal, Chris Chen, Shashi Paruchuri, Lillian Skidmore, Nick Knudsen, Molly Allen.

Project administration: Wayne Yu, Mysore P. Ramprasad.

Supervision: Mysore P. Ramprasad.

Validation: Wayne Yu, Mysore P. Ramprasad, Manoj Pal, Chris Chen, Shashi Paruchuri, Lillian Skidmore, Nick Knudsen, Molly Allen.

Visualization: Wayne Yu, Mysore P. Ramprasad, Manoj Pal.

Writing – original draft: Wayne Yu, Mysore P. Ramprasad.

Writing – review & editing: Wayne Yu, Mysore P. Ramprasad, Lillian Skidmore, Nick Knudsen, Ying Buechler.

References

1. Ferraro E, Drago JZ, Modi S. Implementing antibody-drug conjugates (ADCs) in HER2-positive breast cancer: state of the art and future directions. Breast Cancer Res. 2021 Aug 11; 23(1):84. https://doi.org/10.1186/s13058-021-01459-y PMID: 34380530
2. Jackson D, Atkinson J, Guevara CI, Zhang C, Kery V, Moon SJ, et al. In vitro and in vivo evaluation of cysteine and site specific conjugated herceptin antibody-drug conjugates. PLoS One. 2014 Jan 14; 9 (1):1–14. https://doi.org/10.1371/journal.pone.0083865 PMID: 24454709
3. Nagaraja Shastri P, Zhu J, Skidmore L, Liang X, Ji Y, Gu Y, et al. Nonclinical Development of Next-generation Site-specific HER2-targeting Antibody-drug Conjugate (ARX788) for Breast Cancer Treatment. Mol Cancer Ther. 2020 Sep; 19(9):1822–1832. https://doi.org/10.1158/1535-7163.MCT-19-0692 PMID: 32499302
4. Skidmore L, Sakamuri S, Knudsen NA, Hewet AG, Milutinovic S, Barkho W, et al. ARX788, a Site-specific Anti-HER2 Antibody–Drug Conjugate, Demonstrates Potent and Selective Activity in HER2-low and T-DM1–resistant Breast and Gastric Cancers: Mol Cancer Ther. 2020 Sep; 19(9):1833–1843.
5. Zhang J, Ji D, Shen W, Xiao Q, Gu Y, O'Shaughnessy J, et al. Phase I Trial of a Novel Anti-HER2 Antibody-drug Conjugate, ARX788, for the Treatment of HER2-positive Metastatic Breast Cancer. Clin Cancer Res. 2022 May 26: 0456.2022–2-11. https://doi.org/10.1158/1078-0432.CCR-22-0456 PMID: 35766963
6. Zhang Y, Qiu MZ, Wang JF, Zhang YQ, Shen A, Yuan XL, et al. Phase 1 multicenter, dose-expansion study of ARX788 as monotherapy in HER2-positive advanced gastric and gastroesophageal junction

adenocarcinoma. Cell Rep Med. 2022 Nov 15; 3(11):100814. https://doi.org/10.1016/j.xcrm.2022.100814 PMID: 36384091

7. ICH Q5E, Comparability of Biotechnological/Biological Products Subject to Changes in their Manufacturing Process, June 2005, CPMP/ICH/5721/03. International Conference on Harmonization.
8. Iyer KR, Lequeux I. Risk-Based Approach for Analytical Comparability and Comparability Protocols. PDA J Pharm Sci Technol. 2020 Sep-Oct; 74(5):563–570. https://doi.org/10.5731/pdajpst.2019.010439 PMID: 32295861
9. Chan C. Analytical Strategies for Comparability in Bioprocess Development. BioPharma Asia July/August 2016. P 26–33.
10. Ambrogelly A, Gozo S, Katiyar A, Dellatore S, Kune Y, Bhat R, et al. Analytical comparability study of recombinant monoclonal antibody therapeutics. MAbs. 2018 May/Jun; 10(4):513–538. https://doi.org/10.1080/19420862.2018.1438797 PMID: 29513619
11. Schlegel Mélanie and Bobinnec Yves. Comparability Protocols for Biotechnological Products: A Five-Step Methodology BioProcess Technical June 2013, 11(6), 30–41.
12. Guideline on comparability of biotechnology-derived medicinal products after a change in the manufacturing process: Non-clinical and clinical issues. 19 July 2007 EMEA/CHMP/BMWP/101695/2006 Committee for medicinal products for human use (CHMP), European Medicines Agency.
13. Mihaila R, Ruhela D, Xu L, Joussef S, Geng X, Shi J, et al. Analytical comparability demonstrated for an IgG4 molecule, inclacumab, following transfer of manufacturing responsibility from Roche to Global Blood Therapeutics. Expert Opin Biol Ther. 2022 Nov; 22(11):1417–1428. https://doi.org/10.1080/14712598.2022.2143260 PMID: 36342398
14. Huang RY, Chen G. Characterization of antibody-drug conjugates by mass spectrometry: advances and future trends. Drug Discov Today. 2016 May; 21(5):850–5. https://doi.org/10.1016/j.drudis.2016.04.004 PMID: 27080148
15. Beck A, Terral G, Debaene F, Wagner-Rousset E, Marcoux J, Janin-Bussat MC, et al. Cutting-edge mass spectrometry methods for the multi-level structural characterization of antibody-drug conjugates. Expert Rev Proteomics. 2016; 13(2):157–83. https://doi.org/10.1586/14789450.2016.1132167 PMID: 26653789
16. Beck A, D'Atri V, Ehkirch A, Fekete S, Hernandez-Alba O, Gahoual R, et al. Cutting-edge multi-level analytical and structural characterization of antibody-drug conjugates: present and future. Expert Rev Proteomics. 2019 Apr; 16(4):337–362. https://doi.org/10.1080/14789450.2019.1578215 PMID: 30706723
17. Chen B, Lin Z, Zhu Y, Jin Y, Larson E, Xu Q, et al. Middle-Down Multi-Attribute Analysis of Antibody-Drug Conjugates with Electron Transfer Dissociation. Anal Chem. 2019 Sep 17; 91(18):11661–11669. https://doi.org/10.1021/acs.analchem.9b02194 PMID: 31442030
18. Nowak C, K Cheung J, M Dellatore S, Katiyar A, Bhat R, Sun J, et al. Forced degradation of recombinant monoclonal antibodies: A practical guide. MAbs. 2017 Nov/Dec; 9(8):1217–1230. https://doi.org/10.1080/19420862.2017.1368602 PMID: 28853987
19. Guideline on development, production, characterisation and specification for monoclonal antibodies and related products. 21 July 2016 EMA/CHMP/BWP/532517/2008 Committee for medicinal products for human use (CHMP), European Medicines Agency.
20. Q6B Specifications: Test Procedures and Acceptance Criteria for Biotechnological/Biological Products U.S. Department of Health and Human Services Food and Drug Administration Center for Drug Evaluation and Research (CDER), Center for Biologics Evaluation and Research (CBER). August 1999.
21. Raghavan RR and McCombie R. ICH Q5E Comparability of Biotechnological/Biological Products Subject to Changes in their Manufacturing Process, in: ICH Quality Guidelines An Implementation Guide. Editors, Elder D, Nims R, John Wiley & Sons Inc., 2018. 409–432.
22. Petoskey F, Kwok SC, Jackson W, Jiang S. Overcoming Challenges of Implementing Closed System Transfer Device Clinical In-Use Compatibility Testing for Drug Development of Antibody Drug Conjugates. J Pharm Sci. 2020 Jan; 109(1):761–768. https://doi.org/10.1016/j.xphs.2019.07.021 PMID: 31376374